This full text paper was peer reviewed at the direction of IEEE Communications Society subject matter experts for publication in the ICC 2007 proceedings.

Spectral Efficiency of Channel-Aware Schedulers in Non-identical Composite Links with Interference

Jingxian Wu[†], Neelesh B. Mehta[‡], *Senior Member, IEEE*,
Andreas F. Molisch[‡,*], *Fellow, IEEE*, and Jin Zhang[‡], *Senior Member, IEEE*

***Abstract*— Accurate system planning and performance evaluation requires knowledge of the joint impact of scheduling, interference, and fading. However, current analyses either require costly numerical simulations or make simplifying assumptions that limit the applicability of the results. In this paper, we derive analytical expressions for the spectral efficiency of cellular systems that use either the channel-unaware but fair round robin scheduler or the greedy, channel-aware but unfair maximum signal to interference ratio scheduler. As is the case in real deployments, non-identical co-channel interference at each user, both Rayleigh fading and lognormal shadowing, and limited modulation constellation sizes are accounted for in the analysis. We show that using a simple moment generating function-based lognormal approximation technique and an accurate Gaussian-Q function approximation leads to results that match simulations well. These results are more accurate than erstwhile results that instead used the moment-matching Fenton-Wilkinson approximation method and bounds on the Q function. The spectral efficiency of cellular systems is strongly influenced by the channel scheduler and the small constellation size that is typically used in third generation cellular systems.**

I. Introduction

Next generation cellular communication systems strive to achieve higher spectral efficiencies and deliver higher data rates to users. This needs to be done in the presence of effects such as large-scale fading, which arises due to shadowing, and small-scale fading, which arises due to multipath components, and in an interference-limited environment in which aggressive frequency reuse leads to severe co-channel interference (CCI) from neighboring cells [1]. To achieve the desired high spectral efficiencies, these systems employ advanced techniques such as link adaptation and channel-aware multi-user scheduling. This paper presents a general analysis of the spectral efficiency achievable by these systems, which factors in the interactions between all the above mentioned effects.

Due to its importance in system planning and optimization, the problem of characterizing the spectral efficiency of a cellular system with schedulers has received considerable attention in the literature. The presence of CCI, the competition for radio resources at the scheduler, and the combined effect of fading and shadowing make a system-level (multi-user multi-cell) analysis quite complicated. Given the complexity of analysis, most performance evaluations have been simulation studies [2]–[4], with many of these using very standard-specific models. Analytical spectral efficiency expressions have been obtained as well in the literature but use certain simplifications of the underlying model [5], [6] that limit the accuracy or the applicability of the analysis.

In [5], an analytical framework is developed to quantify the area spectral efficiency of interference-limited cellular systems in the presence of both Rayleigh fading and lognormal shadowing. However, it assumes that the mean power of all the interferers is identical, a situation that does not occur in practical systems. Consequently, the results derived are performance bounds that assume that *all* users are at the best case or worst case locations for interference. The bounds turn out to be quite loose for small reuse distances, at which next generation systems will typically operate. Such an approach also precludes the inclusion of second-tier interference in the analysis. While smaller than first-tier interference, second-tier interference is not negligible. Other related papers are [8] and [9], both of which assume identically distributed interferers and do not consider shadowing. It is also important to note that the results in [5], [8], [9] are only applicable to systems with channel-unaware round robin (RR) schedulers. While [6] does analyze the performance of different schedulers and accounts for multi-tier interference, it makes the simplifying assumption that the throughput equals the signal to interference ratio (SIR) at the receiver. This makes the results applicable only to systems in which the SIR at each mobile is very small. The throughput of different schedulers is also analyzed in [7], but only for a CCI-free single-cell system.

This paper derives general analytical expressions for the spectral efficiency of a cellular system, which do not suffer from any of the above restrictions. We allow for the fact that the interference at each user comes from non-identical co-channel interferers, and that all the links undergo both small-scale Rayleigh fading and large-scale lognormal shadowing. The spectral efficiency of the fair but spectrally inefficient RR scheduler and the unfair but spectrally efficient Max-SIR (signal to interference ratio) scheduler, which schedules to the user with the best instantaneous channel state, is analyzed. The results also serve as lower and upper bounds on the performance of a proportional-fair scheduler [3], which trades off system throughput for fairness. The paper generalizes the analysis in [10], which presented shadowing-conditioned spectral efficiency results, i.e., it only averaged over short-term fading. As we shall see, incorporating shadowing significantly changes the analysis. For example, the differential form of the

[†]Jingxian Wu is with the Dept. of Engineering Science, Sonoma State Univ., Rohnert Park, CA 94928, USA. [‡]Neelesh B. Mehta, Andreas F. Molisch, and Jin Zhang are with the Mitsubishi Electric Research Labs (MERL), 201 Broadway, Cambridge, MA 02139, USA. [*]Andreas F. Molisch is also with Lund Univ., Lund, Sweden. (Emails: jingxian.wu@sonoma.edu, {mehta, molisch, jzhang}@merl.com)

1-4244-0353-7/07/$25.00 ©2007 IEEE

probability distribution function in [10, Lemma 2] that enabled a closed-form analysis is no longer possible.

Our analysis also brings out the significant detrimental effect that a maximum transmission rate limit has on the throughput advantage of Max-SIR schedulers. The maximum transmission rates occur due to small modulation constellations employed in the cellular systems for reasons related to mobile station (MS) complexity and reference signal overhead. For example, 16-QAM is the largest modulation alphabet in the third generation high speed downlink packet access (HSDPA) system, and has a maximum rate of 4 bits/symbol.

The paper is organized as follows. Section II sets up the cellular system model. In Sec. III, statistical properties of the SIR are analyzed, and are used to derive the spectral efficiency of the different schedulers in Sec. IV. Numerical examples in Sec. V are followed by our conclusions in Sec. VI.

II. System Model

Consider a cellular system with N users per cell and multiple cells. In the downlink, each user receives CCI from M neighboring base stations. The received signal at the nth user can be modeled as:

$$r_n = h_{n0}x_{n0} + \sum_{m=1}^{M} h_{nm}x_{nm} + z_n, \tag{1}$$

where x_{n0} is the desired signal with unit power, x_{nm} is the mth interfering signal, and z_n is additive white Gaussian noise. The channel coefficient, h_{nm}, represents the instantaneous complex baseband gain of the channel between the nth user and the mth base station (BS). It can be written as $h_{nm} = \sqrt{\alpha_{nm}}g_{nm}$, where α_{nm} includes the effect of pathloss, shadowing, and sectorization, and the Rayleigh-fading term g_{nm} is a zero-mean, unit-variance complex Gaussian random variable.

The number of interferers, M, depends on the geometric layout of the cellular system and sectorization. For example, for the hexagonal layout shown in Fig. 1, when only first-tier interferers are considered, we have $M = 6$ without sectorization, $M = 2$ for 3 sectors per cell, and $M = 1$ for 6 sectors per cell [11]. When the second-tier interferers are also considered, the corresponding values are $M = 18$, $M = 7$, and $M = 4$.[1]

The probability density function (pdf) of lognormal shadowing is given by

$$f_{\alpha_{nm}}(x) = \frac{\xi}{\sqrt{2\pi}\sigma_{nm}x}\exp\left[-\frac{(\xi\log_e x - \mu_{nm})^2}{2\sigma_{nm}^2}\right], (x \geq 0). \tag{2}$$

where μ_{nm} and σ_{nm}^2 are the mean and variance of the Gaussian random variable (RV), $10\log_{10}\alpha_{nm}$, and $\xi = 10/\log_e 10$.

Specifically, $\mu_{nm} = P_m - L_0 - 10p\log_{10}(d_{nm}/d_0) - A(\theta)$, where P_m is the transmission power (in dBW) of the mth BS, L_0 is the pathloss (in dB) at a reference distance d_0 from the BS, d_{mn} is the distance of the nth MS from the mth BS, p is the pathloss exponent, $A(\theta)$ is the antenna gain (in dB) of the BS, and θ is the angle between the direction of interest and the boresight of the antenna. For example, in [17], $A(\theta)$ is specified as

$$A(\theta) = -\min\left[12\left(\frac{\theta}{\theta_0}\right)^2, A_0\right], -180^{\text{o}} \leq \theta \leq 180^{\text{o}}, \tag{3}$$

where $\theta_0 = 70^{\text{o}}$ and $A_0 = 20$ dB for a 3-sector cell, and $\theta_0 = 35^{\text{o}}$ and $A_0 = 23$ dB for a 6-sector cell. For a 1-sector cell, $A(\theta) = 0$ dB. It is clear from Fig. 1 that the BSs are at different distances from an MS. Therefore, this paper assumes that h_{nm} are independent, but not identically, distributed.

As in [2], [5], [8], [9], we consider a highly spectrally efficient interference-limited scenario in which the noise component is negligible compared to CCI. Neglecting the noise also makes the analysis tractable. The instantaneous SIR, γ_n, of the nth user is

$$\gamma_n = \frac{S_n}{\sum_{m=1}^{M} I_{nm}}, \tag{4}$$

where $S_n = \alpha_{n0}|g_{n0}|^2$ is the desired signal component power, and $I_{nm} = \alpha_{nm}|g_{nm}|^2$ is the CCI from the mth BS.

Spectral efficiency captures the highest data throughput per unit bandwidth achievable by the entire cellular system under the limitations imposed by the system model assumptions. We therefore use the Shannon capacity formula to measure throughput [5], as it is the maximum throughput the channel can reliably support. This also models the case where capacity-achieving error-free codes are used and the transmitter adapts its transmission rates on a continuous scale. The impact of a limited modulation constellation is modeled by means of a cap, $C_{\max} = \log_2(T)$, on the achievable throughput per unit bandwidth:

$$C(\gamma_n) = \begin{cases} \log_2(1+\gamma_n), & \gamma_n \leq \gamma_T \\ C_{\max}, & \gamma_n > \gamma_T \end{cases}, \tag{5}$$

where T is the maximum modulation constellation size allowed in the system, and $C_{\max} = \log_2(1+\gamma_T)$. (Without a constellation size constraint, we have $C_{\max} = \infty$.)

The channel is time-varying. In the spectral efficiency analysis, it is assumed that the schedulers operate at a rate fast enough to adapt to the channel variations. As a result, the instantaneous spectral efficiency $C(\gamma_n)$ varies with time. The average spectral efficiency of the nth user is then

$$C_n = \int_0^\infty C(\gamma) f_{\gamma_n}(\gamma) d\gamma, \tag{6}$$

where $f_{\gamma_n}(\gamma)$ is the pdf of the SIR γ_n.

III. Statistical Properties of SIR

In this section, the statistical properties of the SIR, γ_n, at the receiver of user n are first analyzed. This will facilitate the spectral efficiency analysis that follows.

[1] These values of M arise when the interference from other sectors is neglected. This is justifiable because the antenna pattern attenuates adjacent sector interference by 20 dB or more.

A. Statistics of Signal Component

Due to the combined effects of pathloss, lognormal shadowing, and Rayleigh fading, the received signal power, S_n, follows a composite Rayleigh-lognormal (Suzuki) distribution. The pdf of S_n can be expressed in an integral form as

$$f_{S_n}(x) = \int_0^\infty \frac{1}{y}\exp\left(-\frac{x}{y}\right)\frac{\xi}{\sqrt{2\pi}\sigma_{n0}y} \times \exp\left[-\frac{\left(\xi\log_e y - \mu_{n0}\right)^2}{2\sigma_{n0}^2}\right]dy, \quad (x \geq 0), \quad (7)$$

where μ_{n0} and σ_{n0}^2 are the dB moments of the lognormal RV α_{n0}.

No closed-form formula is available for this composite Rayleigh-lognormal pdf. However, a composite Rayleigh-lognormal RV can be accurately approximated by a new lognormal RV, $\tilde{S}_n \approx S_n$. The dB moments, $\mu_{\tilde{S}_n}$ and $\sigma_{\tilde{S}_n}^2$, of $\tilde{S}_n$ are given by [11, (2.188)]

$$\mu_{\tilde{S}_n} = \xi\cdot\psi(1) + \mu_{n0}, \quad (8a)$$
$$\sigma_{\tilde{S}_n}^2 = \xi^2\cdot\zeta(2,1) + \sigma_{n0}^2, \quad (8b)$$

where $\psi(\cdot)$ is the Euler psi function, and $\zeta(\cdot,\cdot)$ is Riemann's zeta function.

B. Statistics of Sum of Interference Components

The interference power, I_{nm}, from the mth BS is also Suzuki distributed (with its pdf given by (7)). Its dB mean and variance are μ_{nm} and σ_{nm}^2. To evaluate the statistics of the SIR, we need to evaluate the statistics of the sum of M non-identically distributed interference powers, $\sum_{m=1}^{M} I_{nm}$.

It is shown in [12], [13] that a single lognormal RV, $\tilde{I}_n$, can accurately approximate the distribution of the sum of M non-identically distributed composite Rayleigh-lognormal RVs, *i.e.*, $\tilde{I}_n \approx \sum_{m=1}^{M} I_{nm}$. A similar lognormal approximation of the interference power sum was also used in [5], where the approximation was performed in two steps. First, each Suzuki interference component, I_{nm}, is approximated by a lognormal RV, $\tilde{I}_{nm}$. Second, a new lognormal RV, $\tilde{I}_n$, is used to approximate the lognormal sum, $\sum_{m=1}^{M}\tilde{I}_{nm}$, by employing the moment-matching Fenton-Wilkinson (F-W) method [14]. However, this leads to inaccuracies as the F-W method is poor in approximating the head portion (small values of $\tilde{I}_n$) of the sum pdf [12]. This is a problem in an SIR analysis such as ours because $\tilde{I}_n$ is in the denominator of the SIR expression, and its small values do matter. Another source of inaccuracy is that the approximation errors of the two steps accumulate.

We overcome these problems by using the novel, yet simple, moment generating function (MGF)-based method [12], which approximates the sum of non-identical Suzuki RVs by a single lognormal RV directly in one step. More importantly, the method provides the parametric flexibility to handle the inevitable trade-off that needs to be made in approximating different regions of the sum pdf. In Sec. V, we compare the accuracy of the two methods and show that the MGF-based method leads to the most accurate results.

In the MGF-based method, the dB moments, $\mu_{\tilde{I}_n}$ and $\sigma_{\tilde{I}_n}^2$, of $\tilde{I}_n$ are determined by solving the following system of two equations [12]

$$\sum_{k=1}^{K}\frac{w_k}{\sqrt{\pi}}\exp\left[-s_i\exp\left(\frac{\sqrt{2}\sigma_{\tilde{I}_n}a_k + \mu_{\tilde{I}_n}}{\xi}\right)\right] = \prod_{m=1}^{M}\Psi_{I_{nm}}(s_i), \text{ for } i = 1 \text{ and } 2. \quad (9)$$

The left-hand side of the equation is the Gauss-Hermite representation of the MGF of the approximating lognormal RV $\tilde{I}_n$, with K being the Hermite integration order, and $\mu_{\tilde{I}_n}$ and $\sigma_{\tilde{I}_n}$ are the unknowns to be solved for. The weights, w_k, and the abscissas, a_k, are tabulated in [15, Tbl. 25.10]. The right-hand side function, $\Psi_{I_{nm}}(s)$, is the Gauss-Hermite approximation of the Suzuki MGF, and is given by

$$\Psi_{I_{nm}}(s) = \sum_{k=1}^{K}\frac{w_k}{\sqrt{\pi}}\left[1 + s\exp\left(\frac{\sqrt{2}\sigma_{nm}a_k + \mu_{nm}}{\xi}\right)\right]^{-1}, \quad (10)$$

where μ_{nm} and σ_{nm} are the dB mean and dB standard deviation of the lognormal RV α_{nm}, and are known a priori. $\Psi_{I_{nm}}(s)$ only needs to be calculated twice – at s_1 and s_2. The above system of two non-linear equations can be readily solved numerically using standard functions such as `fsolve` in Matlab and `NSolve` in Mathematica. $K = 12$ is sufficient to accurately determine $\mu_{\tilde{I}_n}$ and $\sigma_{\tilde{I}_n}^2$.

In the SIR analysis, $s_1 = 0.2$ and $s_2 = 1.0$ are chosen to give more emphasis to the head portion of the sum pdf [12] because the SIR, which has $\tilde{I}_n$ on the denominator of its expression, is more sensitive to small values of $\tilde{I}_n$.

C. SIR Statistics

With the approximations described above, both the signal power, S_n, and the total interference power, $\sum_{m=1}^{M} I_{nm}$, are approximated by lognormal RVs, $\tilde{S}_n$ and $\tilde{I}_n$, that are independent of each other. Thus, the SIR is now

$$\tilde{\gamma}_n = \frac{\tilde{S}_n}{\tilde{I}_n}, \quad (11)$$

which is also a lognormal RV with parameters

$$\mu_{\tilde{\gamma}_n} = \mu_{\tilde{S}_n} - \mu_{\tilde{I}_n}, \quad (12a)$$
$$\sigma_{\tilde{\gamma}_n}^2 = \sigma_{\tilde{S}_n}^2 + \sigma_{\tilde{I}_n}^2. \quad (12b)$$

Here, $\mu_{\tilde{S}_n}$ and $\sigma_{\tilde{S}_n}^2$ are given by (8), and $\mu_{\tilde{I}_n}$ and $\sigma_{\tilde{I}_n}^2$ can be obtained by solving (9).

The CDF of the lognormally distributed SIR, $\tilde{\gamma}_n$, can then be written in closed-form as

$$F_{\tilde{\gamma}_n}(\gamma) = 1 - Q\left(\frac{10\log_{10}\gamma - \mu_{\tilde{\gamma}_n}}{\sigma_{\tilde{\gamma}_n}}\right), \quad (13)$$

where $Q(x) = \frac{1}{\sqrt{2\pi}}\int_x^{+\infty}\exp(-\frac{y^2}{2})dy$ is the Gaussian-Q function.

IV. Spectral Efficiency Analysis

We now analytically evaluate the average spectral efficiencies of the RR and Max-SIR schedulers. The analysis assumes a full buffer traffic model, in which all users always have data to be transmitted to.

A. Round Robin Scheduler

In a system with the RR scheduler, a user once served by the BS will not be served again until all the other users have been served exactly once. The RR scheduler has the same spectral efficiency as a random scheduler, which schedules all users with the same probability without taking the users' channel states into account. Therefore, the average spectral efficiency, C_{RR}, of the RR scheduler can be shown to be simply the average of all the users' channel-averaged spectral efficiencies, and is given by

$$C_{\text{RR}} = \frac{1}{N}\sum_{n=1}^{N} C_n, \tag{14}$$

where N is the number of active users in the system, and C_n is the average spectral efficiency of the nth user. Note that an equation similar to (14) was in [5], [8], [9] to calculate the average spectral efficiency. Consequently, their results only apply to the RR scheduler.

The average spectral efficiency of the nth user is obtained by substituting (5) into (6):

$$C_n = \log_2 e \int_0^{\gamma_T} \frac{1}{1+\gamma}\left[1 - F_{\gamma_n}(\gamma)\right] d\gamma, \tag{15}$$

where γ_T is the SIR threshold related to the modulation constellation size limit, as described in (5). Combining (13)–(15) leads to the following formula for the average spectral efficiency of a system with the RR scheduler:

$$C_{\text{RR}} = \frac{\log_2 e}{N}\int_0^{\gamma_T} \frac{1}{1+\gamma}\sum_{n=1}^{N} Q\left(\frac{\xi \log_e \gamma - \mu_{\tilde{\gamma}_n}}{\sigma_{\tilde{\gamma}_n}}\right) d\gamma. \tag{16}$$

Since the Gaussian-Q function is defined in the form of an integral, the evaluation of the average spectral efficiency given in (16) effectively requires a two-fold integration. This can be simplified by using the following very accurate approximation of the Gaussian-Q function [16]

$$\hat{Q}(x) = \frac{\exp\left(-x^2/2\right)}{1.64x + \sqrt{0.76x^2+4}}, \text{ for } x \geq 0. \tag{17}$$

The relative variation, $\left|\hat{Q}(x) - Q(x)\right| / Q(x)$, is smaller than 0.3% for $x > 0$. Using the relationship $Q(x) = 1 - Q(-x)$, for $x < 0$, we can simplify the representation of C_{RR} by combining (16) and (17). The final expression for the spectral efficiency is given in (18) in terms of an easily computable single finite integral with only elementary functions in its integrand.

In [5], the numerical complexity was avoided by using an upper bound and a lower bound of the function $\log_2(1+\gamma)$. The bounds are loose for small reuse distances. The approximation of $\log_2(1+\gamma) \approx \gamma$ was adopted in [6] to simplify the spectral efficiency analysis. This approximation only applies to smaller value of γ. Using the Gaussian-Q function approximation of (17) instead leads to a more accurate characterization of the SIR over a wider range of its values, while also simplifying the numerical computation.

B. Max-SIR Scheduler

Compared to the RR scheduler, the Max-SIR scheduler improves throughput by always serving the user with the highest SIR. As mentioned, these gains come at the expense of fairness and also an increased feedback overhead. Unlike the RR scheduler, the Max-SIR scheduler requires the BS to know the channel gains of all the MSs.

Let $\gamma_{\max} = \max\{\tilde{\gamma}_1, \tilde{\gamma}_2, \cdots, \tilde{\gamma}_N\}$ denote the maximum SIR among the N users at any instant. The average spectral efficiency of a system with the Max-SIR scheduler can then be written as [c.f. (15)]

$$C_{\text{MSIR}} = \log_2 e \int_0^{\gamma_T} \frac{1}{1+\gamma}\left[1 - F_{\gamma_{\max}}(\gamma)\right] d\gamma, \tag{19}$$

where $F_{\gamma_{\max}}(\gamma)$ is the CDF of the maximum SIR, $\gamma_{\max}$. From (13), $F_{\gamma_{\max}}(\gamma)$ is given by

$$\begin{aligned} F_{\gamma_{\max}}(\gamma) &= P(\tilde{\gamma}_1 < \gamma, \tilde{\gamma}_2 < \gamma, \cdots, \tilde{\gamma}_N < \gamma), \\ &= \prod_{n=1}^{N}\left[1 - Q\left(\frac{\xi \log_e \gamma - \mu_{\tilde{\gamma}_n}}{\sigma_{\tilde{\gamma}_n}}\right)\right], \end{aligned} \tag{20}$$

where the second equality follows because the SIRs $\{\tilde{\gamma}_n\}_{n=1}^{N}$ are independent.

From (19) and (20), the average spectral efficiency of the Max-SIR scheduler after averaging over both Rayleigh fading and lognormal shadowing is

$$\begin{aligned} C_{\text{MSIR}} &= \log_2(e) \\ &\times \int_0^{\gamma_T} \frac{1}{1+\gamma}\left(1 - \prod_{n=1}^{N}\left[1 - Q\left(\frac{\xi \log_e \gamma - \mu_{\tilde{\gamma}_n}}{\sigma_{\tilde{\gamma}_n}}\right)\right]\right) d\gamma. \end{aligned} \tag{21}$$

As before, the average spectral efficiency expression can be further simplified as before by using (17). The details are omitted due to space constraints.

The spectral efficiency expressions given in (18) and (21) are also applicable to systems operating in an environment with only lognormal shadowing and no (or minimal) Rayleigh fading. This can occur in the presence of a line-of-sight connection, or in transceivers that use micro-diversity (e.g., antenna diversity or frequency diversity) to eliminate small-scale fading. In such cases, the only change in the average spectral efficiency evaluation is the re-computation of the dB moments, $\mu_{\tilde{\gamma}_n}$ and $\sigma^2_{\tilde{\gamma}_n}$, of the SIR.

V. Numerical Examples

A representative hexagonal cellular layout, shown in Fig. 1, with a reuse factor of 1 and with up to two tiers of interfering BSs is used in the results below. The pathloss exponent is assumed to be 3.7. Unless otherwise mentioned, the dB standard deviation of all lognormal RVs is $\sigma = 8$ and the number of sectors per cell is one.

$$\widetilde{C}_{\text{RR}} = \frac{\log_2 e}{N} \sum_{n=1}^{N} \left[\log_e \left(1 + e^{\mu_{\tilde{\gamma}_n}/\xi} \right) - \int_0^{\gamma_T} \frac{\sigma_{\tilde{\gamma}_n} \exp\left(- \left| \xi \log_e \gamma - \mu_{\tilde{\gamma}_n} \right|^2 / 2\sigma_{\tilde{\gamma}_n}^2 \right) / (1+\gamma)}{1.64 \left| \xi \log_e \gamma - \mu_{\tilde{\gamma}_n} \right| + \sqrt{0.76 \left| \xi \log_e \gamma - \mu_{\tilde{\gamma}_n} \right|^2 + 4\sigma_{\tilde{\gamma}_n}^2}} d\gamma \right]. \quad (18)$$

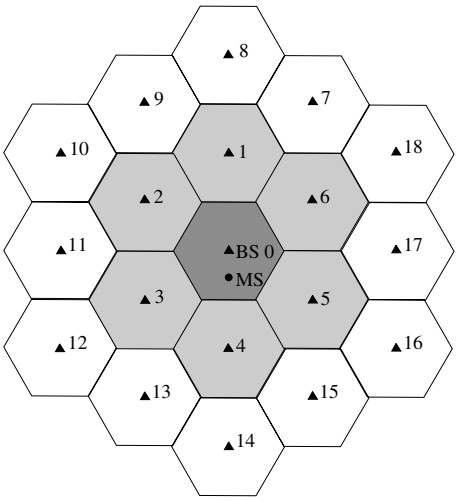

Fig. 1. Hexagonal layout of a 19-cell cellular system.

We first study the case where there is no limit on the modulation constellation. Figure 2 plots the average spectral efficiency per cell of a system with 10 users per cell when only the interference from the first-tier interfering BSs is considered. To ensure a fair comparison between the RR and Max-SIR schedulers, all the users are distributed on a circle centered at the serving BS.[2] Note, however, that the analysis presented in this paper can handle arbitrary user locations. It can be seen from Fig. 2 that the analytical results agree with the simulation results very well for both the schedulers. This results demonstrate the accuracy of using the MGF-based Suzuki sum approximation and the Gaussian-Q function approximation in the analysis. Also plotted are the analytical results obtained with the F-W lognormal approximation method. These deviate from the simulation results due to the inaccuracy of the F-W method.

The average spectral efficiencies of the Max-SIR and RR schedulers are plotted in Fig. 3 as a function of the number of users per cell, N. Multiple-tier interference is now considered. All the users are at a distance of a half cell radius from the serving BS. As expected, the spectral efficiency of the RR scheduler is independent of N, whereas the spectral efficiency of the Max-SIR scheduler increases monotonically with N – thanks to multi-user diversity. Neglecting the second-tier interferers overestimates the spectral efficiency by 20% for a RR scheduler, and by 8% for a Max-SIR scheduler.[3]

Figure 4 illustrates the effects of cell sectorization and σ on the average spectral efficiency of the Max-SIR scheduler. Ten users per cell are considered, with all users being on a circle with a radius half the cell radius. The antenna pattern in (3) is used. It can be seen that sectorization benefits system performance by reducing the number of co-channel interferers. Performance improves by approximately 87% and 33% when the number of sectors increases from 1 to 3, and from 3 to 6, respectively. In addition, for the Max-SIR scheduler, a larger σ leads to a higher spectral efficiency. This is intuitive, as a larger variance of the channel gain increases the possible multiuser diversity gain. Note that the simulation results and the analytical results agree very well in Figs. 3 and 4.

The impact of the modulation constellation size limit on the average spectral efficiency is illustrated in Fig. 5, for both the schedulers. As before, the number of users per cell is $N = 10$, with all the users placed at the same distance from BS. It is interesting to note that while the Max-SIR scheduler always outperforms the RR scheduler, the modulation constellation size limit undercuts its throughput advantage. Again, this is intuitive, as the user with the best SIR has a very high instantaneous capacity, which it cannot exploit if the modulation alphabet size is restricted. This is especially so when the users are closer to the serving BS. At the cell edge, the impact of the constellation size limit is limited due to greater interference.

VI. Conclusions

We analyzed the system-level spectral efficiency of interference-limited cellular systems that use either the round robin or the Max-SIR schedulers. The analysis is sufficiently general to include the combined effects of Rayleigh fading, lognormal shadowing, channel-aware scheduling, limited modulation constellation, and non-identical co-channel interference. It avoids the simplifying assumption about the placement of interferers and includes the effect of multiple tiers of interferers. The use of a novel MGF-based lognormal approximation method and an accurate approximation of the Gaussian-Q function eliminated the remaining discrepancies between analysis and simulation results that were encountered in the literature. The modulation constellation size limit diminishes the throughput gains of the Max-SIR scheduler, especially when the users are close to the serving base station. Multiple tier interference has a greater impact on the performance of the RR scheduler than the Max-SIR scheduler. The analytical results in this paper thus provide a benchmark against which the results of system-level simulators can be compared. Future work includes extending the analysis to proportional fair schedulers.

[2] This ensures that all users still get served for the same time, on average, even with the Max-SIR scheduler.

[3] Intuitively, second-tier interference will matter less as the noise power, which is neglected in our analysis, increases relative to interference power.

References

[1] A. F. Molisch, "Wireless Communications," IEEE Press – Wiley, 2005.

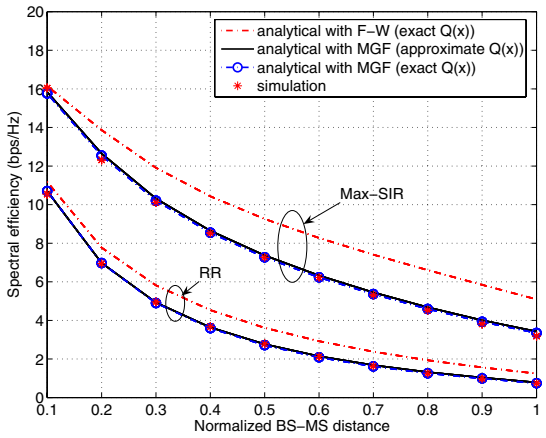

Fig. 2. Comparison of spectral efficiency results from analysis (using different lognormal approximation methods) and simulations for the RR and Max-SIR schedulers.

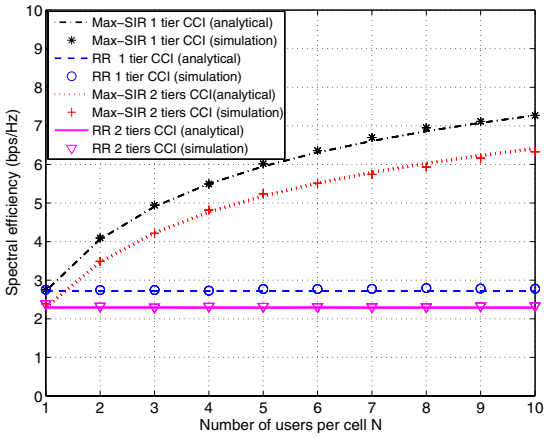

Fig. 3. Spectral efficiency of the RR and Max-SIR schedulers for different numbers of users and multiple tiers of co-channel interferers.

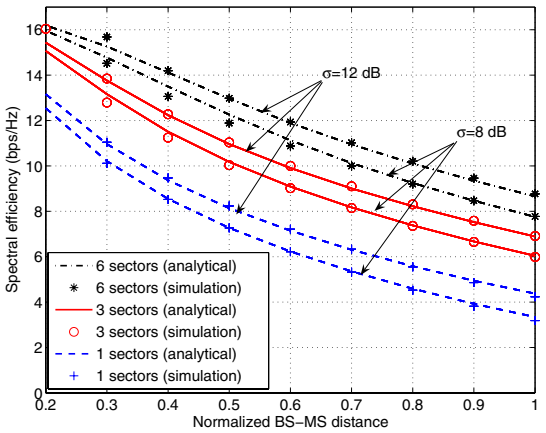

Fig. 4. Spectral efficiency of the Max-SIR scheduler with different cell sectorizationss and shadowing dB standard deviations, σ.

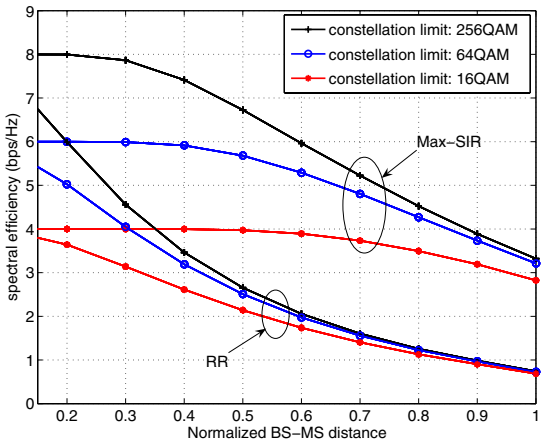

Fig. 5. Spectral efficiency of the RR and Max-SIR schedulers with different modulation constellation size limits.

[2] S. Catreux, P. F. Driessen, and L. J. Greenstein, "Simulation results for an interference-limited multiple-input multiple-output cellular system," *IEEE Commun. Lett.*, vol. 4, pp. 334–336, Nov. 2000.

[3] A. Jalali, R. Padovani, and R. Pankaj, "Data throughput of CDMA-HDR a high efficiency-high data rate personal communication wireless system," in *Proc. IEEE Veh. Technol. Conf. (Spring)*, pp. 1854–1858, May 2000.

[4] J. Ramiro-Moreno, K. I. Pedersen, and P. E. Mogensen, "Network performance of transmit and receive antenna diversity in HSDPA under different packet scheduling strategies," in *Proc. IEEE Veh. Technol. Conf. (Spring)*, pp. 1454–1458, May 2003.

[5] M.-S. Alouini, and A. J. Goldsmith, "Area spectral efficiency of cellular mobile radio systems," *IEEE Trans. Veh. Technol.*, vol. 48, pp. 1047–1066, July 1999.

[6] H. Fu and D. I. Kim, "Analysis of throughput and fairness with downlink scheduling in WCDMA networks," *IEEE Trans. Wireless Commun.*, vol. 5, pp. 2164-2174, Aug. 2006.

[7] A. Senst, P. Schulz-Rittich, G. Ascheid, and H. Meyr, "On the throughput of proportional fair scheduling with opportunistic beamforming for continuous fading states," in *Proc. IEEE Veh. Technol. Conf. (Fall)*, pp. 300–304, Sept. 2004.

[8] M. O. Hasna, M.-S. Alouini, A. Bastami, and E. S. Ebbini, "Performance analysis of cellular mobile systems with successive co-channel interference cancellation," *IEEE Trans. Wireless Commun.*, vol. 2, pp. 29–40, Jan. 2003.

[9] M, Kang, M.-S. Alouini, and L. Yang, "Outage probability and spectrum efficiency of cellular mobile radio systems with smart antennas," *IEEE Trans. Commun.*, vol. 50, pp. 1871–1877, Dec. 2002.

[10] J. Wu, N. B. Metha, J. Zhang, "Spectral efficiency analysis of cellular systems with channel-aware schedulers," in *Proc. IEEE Global Telecommun. Conf. Globecom'05*, vol. 3, pp. 1383–1387, Nov. 2005.

[11] G. L. Stüber, *Principles of Mobile Communications*. Kluwer Academic Publishers, 1996.

[12] N. B. Mehta, A. F. Molisch, J. Wu, and J. Zhang, "Approximating the sum of correlated lognormal or lognormal-rice random variables," in *Proc. IEEE Intern. Conf. Commun.*, pp. 1605–1610, Jun. 2006.

[13] F. Graziosi and F. Santucci, "On SIR fade statistics in Rayleigh-lognormal channels," in *Proc. IEEE Intern. Conf. Commun.*, vol. 3, pp. 1352–1357, May 2002.

[14] L. F. Fenton, "The sum of lognormal probability distributions in scatter transmission systems," *IRE Trans. Commun. Syst.*, vol. CS-8, pp. 57–67, 1960.

[15] M. Abramowitz and I. Stegun, *Handbook of mathematical functions with formulas, graphs, and mathematical tables*. Dover, 9th ed., 1972.

[16] N. Kingsbury, "Approximation formulae for the Gaussian error integral, $Q(x)$," *The connexions project,* http://cnx.org/content/m11067/latest, June 2005.

[17] "Spatial channel model for multiple input multiple output (MIMO) simulations," Tech. Rep. 25.996, 3rd Generation Partnership Project (3GPP).